PCCP

PAPER

View Article Online
View Journal | View Issue



Cite this: *Phys. Chem. Chem. Phys.*, 2016, **18**, 12541

# Solid-state NMR and DFT predictions of differences in COOH hydrogen bonding in odd and even numbered *n*-alkyl fatty acids†

Jacob Powell, Keyton Kalakewich, Fernando J. Uribe-Romo and James K. Harper*

For nearly 140 years *n*-alkyl monocarboxylic acids have been known to exhibit unusual non-monotonic melting between odd and even numbered acids. This behavior has been rationalized in terms of packing density at the hydrocarbon tails, with COOH hydrogen bonding considered to be invariant among different acids. A recent ambiguity involving the COOH conformation between two crystal structures of lauric acid suggests that COOH structure and hydrogen bonding may play a role in these differences. Here, the two conflicting lauric acid crystal structures are further refined using lattice-including DFT refinement methods. Solid-state NMR (SSNMR) $^{13}$C chemical shift tensor data are employed to monitor refinement quality by comparing experimental and computed tensors. This comparison provides a more sensitive measure of structure than X-ray data due to SSNMR's ability to accurately locate hydrogens. Neither diffraction structure agrees with SSNMR data and an alternative is proposed involving a hydrogen disordered COOH moiety. The disordered hydrogen dynamically samples two most probable positions on the NMR timescale with O–H bond lengths of 1.16 and 1.46 Å. This disordered structure is consistent with SSNMR, IR and X-ray C–O and C=O bond lengths. The hydrogen disorder appears to be restricted to even numbered acids based on undecanoic acid's $^{13}$COOH tensor data and C–O and C=O bond lengths for other *n*-alkyl acids. This disorder in even numbered acids results in stronger hydrogen bonds than are found in odd acids and invites a reevaluation of the melting behavior of *n*-alkyl acids that includes these differences in hydrogen bonding.

Received 19th January 2016,
Accepted 7th April 2016

DOI: 10.1039/c6cp00416d

www.rsc.org/pccp



## Introduction

Lauric acid is a twelve carbon *n*-alkyl monocarboxylic acid (Fig. 1A) occurring naturally in certain plant oils[1–4] and in the milk of some mammals.[5] Lauric acid's long-studied influence on human health and diet together with its well-known antimicrobial activity[6,7] has made it the focus of a vast number of studies. While much of this work centers on lauric acid's properties and behavior in solution, there is also interest in lauric acid in the solid state where it exhibits polymorphism, with 5 known phases.[8–14] Phase C,[15] which occurs immediately before melting, is of particular interest, in part, because lauric acid has a high enthalpy of fusion and may therefore be useful as a thermal energy storage material.[16,17] Of perhaps greater general interest is the fact that solid *n*-alkyl monocarboxylic acids present an intellectual puzzle that has intrigued scientists for over a century. As the number of carbons in these acids increase, an unusual non-monotonic increase in melting point is observed with the even numbered acids melting at higher temperatures.[18] Densities, sublimation enthalpies and solubilities also exhibit this behavior with even numbered acids showing higher values.[12] Crystallography has been employed to elucidate this unusual behavior and this work has resulted in the publication of reasonably accurate crystal structures for most of these acids. Curiously, lauric acid is an exception where two crystal structures have recently been reported for phase C and these structures disagree on the orientation of the COOH moiety. The single crystal X-ray structure[13] specifies a *trans* orientation having a O=C–Cα–Cβ dihedral angle of 180° while the X-ray powder structure[12] indicates a *cis* orientation with an angle of 0° (Fig. 1B and C).

Recent studies have demonstrated that SSNMR provides an extremely sensitive way to monitor crystal structure refinements.[19–29] These SSNMR investigations accurately locate hydrogens in many cases and therefore provide a critical piece of structural information often lacking in X-ray diffraction. These refinement studies typically employ DFT methods that account for lattice effects (*e.g.* CASTEP[30]). Improvement is indicated by better agreement between experimental and

*Department of Chemistry, University of Central Florida, 4111 Libra Drive, Orlando, Florida, 32816, USA. E-mail: James.Harper@ucf.edu*

† Electronic supplementary information (ESI) available. See DOI: 10.1039/c6cp00416d

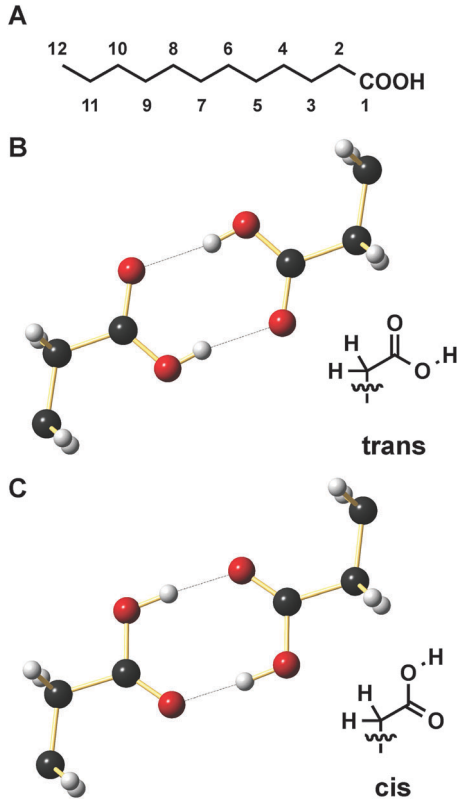


Fig. 1 (A) Lauric acid showing the numbering used herein. Differences in the *trans* and *cis* orientations involve a 180° rotation about the O=C–Cα–Cβ dihedral angle as illustrated by structures (B) and (C), respectively.

calculated SSNMR parameters and a decrease in forces on the atoms of the lattice. In a few cases, where a high quality reference structure is independently known[23–25,29] (*e.g.* single crystal neutron diffraction of the same phase), it has been demonstrated that these refinements consistently create coordinates that are in better agreement with the reference structure than were the original unrefined values. This SSNMR work is of considerable interest because it offers an experimentally verified non-diffraction method for further improving low-resolution structures in a manner that provides accurate coordinates for all atomic sites including hydrogens.

One of the challenges to current DFT refinement studies is the observation that, while large changes are observed in the computed SSNMR parameters, only small movements occur in most atom positions. Indeed, in many of the structures studied, the new atomic positions lie within the error reported for the original diffraction coordinates. Questions thus arise about whether such refinements can actually lead to new insights. Recent work has demonstrated that, at least in a few cases, new insights can be obtained. For example, refinement of the structure of cellulose $I_\alpha$[31] clarified the hydrogen bonding arrangement at 4 positions and eliminated an alternative hydrogen-bonding scheme thought to be feasible based on diffraction data.[32] A second study demonstrated that refinement could establish coordinates of atoms that were missed in a diffraction study of a pentapeptide.[33] This result is of particular interest because high-resolution data is difficult to obtain for many proteins and nucleic acids. Here, DFT and other refinement methods are employed to reconcile the differences found in lauric acid's crystal structures. In this case, refinement of a single hydrogen in lauric acid's crystal structure significantly improves agreement with SSNMR shift tensor data and provides new understanding into differences in hydrogen bonding in *n*-alkyl monocarboxylic acids.

## Experimental

Lauric acid was purchased from Aldrich and prepared in the C form by melting the solid and then quenching it in liquid nitrogen. The resulting solid was gently ground to prevent a phase change and this powder was used for all solid-state NMR analyses.

An X-ray powder diffraction was conducted to ensure that the lauric acid powder obtained from the melt was phase C ($P2_1/c$, monoclinic).[13] Analysis was performed using a Rigaku Miniflex 600 diffractometer, with $\theta$–$2\theta$ Bragg–Brentano geometry, and a 600 W (40 kV, 15 mA) Cu X-ray tube source using Kα ($\lambda$ = 1.5418 Å) radiation. Samples were measured from $2\theta$ = 4 to 40° using a step size of 0.02° and a scan rate of 1.5 s per step. Samples were prepared by placing the powder on a glass sample holder. The powder pattern obtained closely matched the pattern derived from prior X-ray diffraction studies.[12,13] Phases other than phase C exhibit large differences in their powder patterns, thus a visual comparison of the powder pattern was sufficient to clearly distinguish phase C from alternative polymorphs.

A five-pi replicated magic angle turning (FIREMAT)[34] analysis was performed on the C phase of lauric acid in order to obtain $^{13}$C tensor principal values. FIREMAT data was acquired on a Chemagnetics CMX400 spectrometer using 7.5 mm PENCIL probe and operating at a frequency of 100.61916 MHz. Acquisition parameters included evolution and acquisition spectral widths of 26.9 and 65.4 kHz, respectively, a recycle time of 20 s, pulse widths of 4.5 and 9.4 μs for the $^1$H 90° and $^{13}$C 180° pulses, respectively, a 3 ms cross-polarization time, spinning speed of 527 Hz, decoupler frequency of 400.18800 MHz and a TPPM[35] phase angle of 33.6°. The spectrum was externally referenced to the methyl resonance of hexamethyl benzene at 17.35 ppm. A total of 51 evolution dimension increments were acquired of 192 transients each. The digital resolution of the acquisition dimension was 16.0 Hz per point. The evolution dimension was significantly extended using a data rearrangement process described elsewhere[34] to ultimately provide a digital resolution of 16.0 Hz per point. The FIREMAT data were TIGER[36] processed.

The $^{13}$C chemical shift tensor for the COOH moiety in undecanoic acid phase C′ [15] was measured on an Agilent DD2 500 MHz narrow-bore spectrometer operating at 125.68166 MHz with an Agilent 1.6 mm T3 probe. Acquisition parameters for this 1D spectrum included a spectral width of 50.0 kHz, a 3.0 ms cross-polarization time, a $^1$H proton pulse width of 1.0 μs, a digital resolution was 48.8 Hz per point, and SPINAL decoupling

 

at a $^{1}$H frequency of 499.77670. The spectrum was externally referenced to the methyl resonance of hexamethyl benzene at 17.35 ppm. Analysis was conducted at 23 °C using a non-spinning sample and a 25 s recycle time because phase C′ has stability over only a small temperature range of 17.2 °C to 28.5 °C[37] and the risk of melting the sample or inducing a phase change by spinning or pulsing too quickly was considered high. The $^{13}$COOH powder pattern was completely resolved from all other signals allowing principal values to be determined by visually inspecting the spectrum. The error in principal values is estimated to be ±2 ppm based on the width of the singularities representing the principal values in the powder pattern.

An X-ray powder diffraction analysis was conducted on undecanoic acid to verify that the powder utilized was phase C′ ($P2_1/c$, monoclinic).[13] All analysis conditions are identical to those described above for lauric acid. The observed powder pattern closely matched a pattern derived from the prior single-crystal diffraction study.[13]

All $^{1}$H/$^{13}$C heteronuclear correlation (HETCOR) spectra[38] were acquired on an Agilent DD2 500 MHz narrow-bore spectrometer operating at 125.68166 MHz together with an Agilent 1.6 mm T3 probe. Acquisition parameters include acquisition and evolution dimension spectral widths of 29.8 kHz and 14.0 kHz, respectively, 128 evolution increments of 64 transients each, a recycle time of 16 s, and a spinning speed of 12.0 kHz. SPINAL decoupling[39] was used for all spectra using a frequency of 499.77528 MHz and a 165° pulse of 1.84 μs. Each evolution step employed a $^{1}$H frequency offset of ±175.0 kHz and 360° pulse widths of 3.3 μs. A series of HETCOR spectra were acquired using Lee-Goldburg cross-polarization[40] and contact times of 100 μs, 200 μs, 300 μs and 400 μs. All other acquisition parameters are as listed above. The $^{13}$C dimensions of all spectra were externally referenced to the methyl peak in hexamethyl benzene at 17.35 ppm. The $^{1}$H dimensions of all spectra were externally referenced to a non-spinning sample of liquid DMSO in a sealed capillary with a resonance at 2.49 ppm. All $^{1}$H shifts were scaled by 0.577 as required for optimal Lee-Goldburg decoupling.[40]

The isotropic $^{1}$H chemical shift of the COOH moiety in lauric acid phase C was measured by acquiring a 1D spectrum on an Agilent DD2 500 MHz narrow-bore spectrometer operating at 499.77528 MHz. An Agilent 1.6 mm T3 probe was employed and data was acquired at a spinning speed of 25.0 kHz. Other acquisition parameters included a 1.0 μs 90° pulse width, a spectral width of 147.1 kHz and a recycle time of 20.0 s. The spectrum was externally references to a non-spinning sample of liquid dimethyl sulfoxide sealed in a glass capillary with a $^{1}$H resonance at 2.49 ppm.

An elemental analysis of lauric acid phase C gave %C = 71.88, %O = 16.13, and %H = 12.10 *versus* theoretical values of %C = 71.95, %O = 15.97, %H = 12.08. All analyses were performed at Atlantic Microlab, Inc. and are reported to have an uncertainty of ±0.3%.

All geometry refinement and NMR tensor calculations were performed at the University of Central Florida's Advanced Research Computing Center (ARCC). Both of lauric acid's crystal structures were initially refined using the planewave DFT code CASTEP together with the PBE functional and ultra-soft pseudopotentials. The ''ultra-fine'' level was selected using a planewave basis set cut-off energy of 610 eV. The threshold convergence for SCF tolerance was $5 \times 10^{-7}$ eV per atom and a *k*-point spacing of 0.071 Å$^{-1}$ was employed. The minimizing approach of Pfrommer *et al.*[41] was used for geometry optimizations. Optimizations were considered converged when a change in energy threshold of $5 \times 10^{-6}$ eV per atom was reached, a maximum Cartesian force of 0.01 eV Å$^{-1}$ on all atoms was achieved, and the maximum displacement of $5 \times 10^{-4}$ Å for each atom was observed. The unit cell dimensions from the single crystal[13] and powder diffraction[12] studies agree within 1% with respective values of $a$ = 27.563 Å, $b$ = 4.9627 Å, $c$ = 9.5266 Å, $\beta$ = 98.006° and $a$ = 27.54 Å, $b$ = 4.953 Å, $c$ = 9.604 Å, $\beta$ = 97.28°. The DFT methods employed are known to overestimate these parameters,[19] thus refinement of both structures did not include adjustment of unit cell parameters. After geometry refinement, lattice-including NMR calculations were performed (PBE/ultrafine) using the gauge including projector augmented wave (GIPAW)[42] method.

Model structures were prepared involving a pair of butyric acid molecules to evaluate COOH hydrogen positions. Butyric acids were manually placed in a $R_2^2(8)$ hydrogen bonding arrangement. Non-hydrogen atoms were placed at positions determined from lauric acid's single crystal diffraction structure. All hydrogens in C–H bonds were located from the CASTEP geometry refinement as described above. The COOH hydrogens were placed at a series of positions ranging from 1.0 to 1.7 Å in steps ranging in size from 0.03–0.1 Å and $^{13}$C NMR shift tensors computed at the B3LYP/D95** level of theory for each structure without further geometry optimization. The resulting computed shieldings for the COOH carbons were converted to shifts using previously established[43] slope and intercept values of 1.01 and 194.93 which have been found to give accurate shifts for many sp$^2$ carbons.

The influence of disorder on hydrogen bond strength was evaluated by calculating the COOH $^{1}$H chemical shielding tensor at a series of O–H separation distances ranging from 1.0–1.7 Å in steps of 0.1 Å. All calculations were performed at the B3LYP/D95** level of theory using the butyric acid dimer model described above. The $^{1}$H shielding values for tetramethyl silane were also computed (B3LYP/D95**) after geometry optimization (B3LYP/D95*) and employed as a reference to convert shieldings to shifts.

## Results and discussion

A wide variety of SSNMR parameters have now been utilized to monitor the refinement of crystal structure.[19,21–24,42,44–46] Among these, the chemical shift tensor principal values have been reported to be one of the more sensitive parameters,[47] in part because three shifts are measured for each nuclear position. Accordingly, $^{13}$C shift tensors were acquired for lauric acid using the FIREMAT[34] tensor measurement experiment.

Table 1 Experimental $^{13}C$ chemical shift tensor principal values for lauric acid

| Position | $\delta_{11}$ (ppm) | $\delta_{22}$ (ppm) | $\delta_{33}$ (ppm) | $\delta_{iso}$ (ppm) |
|---|---|---|---|---|
| 1[a] | 238.8 | 199.4 | 107.6 | 181.9 |
| 2[a] | 55.9 | 42.7 | 8.0 | 35.5 |
| 3[a] | 37.0 | 28.2 | 9.8 | 25.0 |
| 4[a] | 49.0 | 35.6 | 11.7 | 32.1 |
| 5 | 52.4 | 36.8 | 13.1 | 34.1 |
| 6[b] | 49.1 | 35.6 | 13.1 | 32.6 |
| 7[b] | 50.8 | 36.6 | 13.0 | 33.5 |
| 8[b] | 50.8 | 36.6 | 13.0 | 33.5 |
| 9[b] | 50.2 | 36.2 | 13.2 | 33.2 |
| 10 | 52.8 | 39.2 | 12.9 | 35.0 |
| 11[a] | 35.7 | 28.0 | 12.7 | 25.5 |
| 12[a] | 24.0 | 20.0 | 2.0 | 15.3 |

[a] Experimentally determined from $^{1}H/^{13}C$ correlation experiments. [b] Assigned are interchangeable.

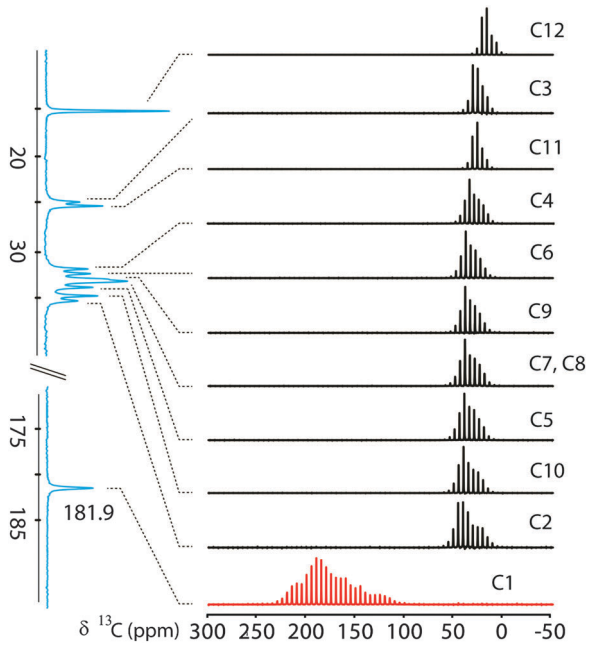


Fig. 2 The $^{13}C$ FIREMAT spectrum obtained for lauric acid, phase C. A total of 11 lines were resolved in the isotropic spectrum (blue) and high signal-to-noise powder patterns obtained for each line to provide tensors. Black patterns indicate $sp^3$ sites while red denotes the COOH.

A total of 11 isotropic resonances were resolved and corresponding tensors obtained for all lines (Table 1). An illustration of the FIREMAT spectrum obtained is given in Fig. 2. All resonances were assigned to molecular positions by a process described in ESI.†

When multiple crystal structures have been reported for the same phase, lattice-including DFT refinements usually reconcile structural differences and cause convergence to a single structure.[24,25] It was therefore hypothesized that the differences in lauric acids COOH structure would be resolved by refinement. Both of lauric acid's crystal structures were therefore refined and $^{13}C$ tensors computed using lattice-including DFT methods (see Experimental). This process significantly improved agreement between computed and experimental tensors at $CH_2$

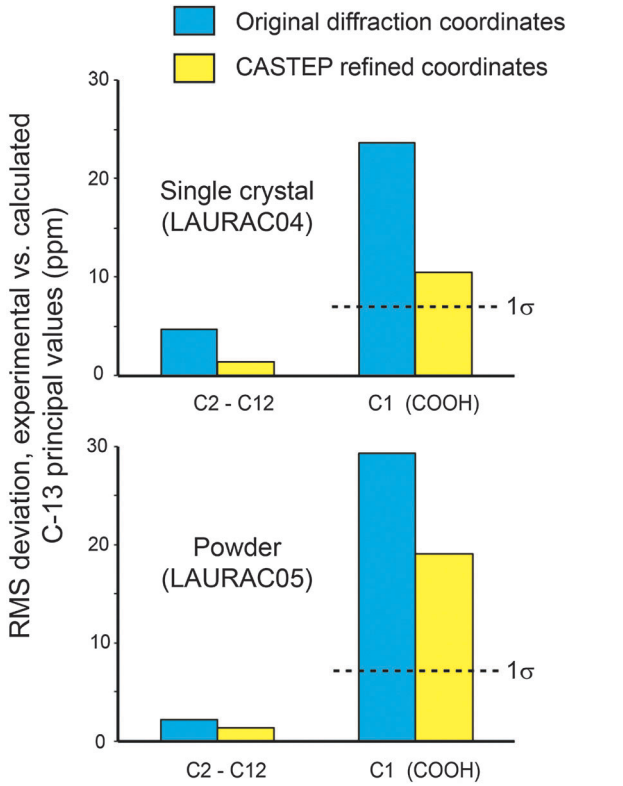


Fig. 3 The root-mean-squared difference (rmsd) between calculated and experimental NMR $^{13}C$ tensors before (blue) and after (yellow) refinement. The fit at $sp^3$ sites is significantly better than the agreement at the $sp^2$ (COOH) position. The expected error at $^{13}COOH$ moieties in well-defined structures is approximately 7.0 ppm (indicated by the $1\sigma$ dashed line) based on independent lattice-including computations of the $^{13}COOH$ tensors in geometry refined structures of formic and acetic acid. These data suggest that neither the X-ray single crystal nor the powder diffraction structures of lauric acid are correct at the COOH moiety.

and $CH_3$ positions (*i.e.* C2–C12). In fact, the agreement at all $sp^3$ sites after refinement is comparable to the expected experimental error,[47] suggesting that the structure at C2–C12 is correct. In contrast, the COOH conformation in both refined structures remained unchanged and each $^{13}COOH$ gave poor agreement with experimental data. Fig. 3 illustrates agreement between experimental and calculated NMR tensors (root-mean-squared difference, rmsd) before and after refinement. The poor fit at the COOH may indicate that both the *cis* or *trans* structures are incorrect or may simply reflect a greater difficulty in calculating accurate shift tensors at COOH moieties. To distinguish between these two possibilities, $^{13}C$ shift tensors were computed for the COOH sites in formic and acetic acid. These model compounds have well-established crystal structures[48,49] with COOH hydrogens purported to be localized. Of equal importance is the fact that the $^{13}C$ shift tensor data is known for both molecules.[50,51] The geometry of both crystal structures was refined and $^{13}C$ tensors calculated using the lattice-including methods employed for lauric acid. An rmsd of 7.0 ppm was observed at the $^{13}COOH$ in the model compounds. The corresponding rmsd in the *cis* structure of lauric acid was 18.7 ppm, eliminating it as a feasible structure. The *trans* structure with an rmsd of 10.5 ppm is also

 

improbable with an rmsd falling outside of 86.6% of a Gaussian distribution (*i.e.* 1.5 standard deviations). The poor fit at both the *cis* and *trans* structures suggests that other structural models should be considered for the COOH. However, it is notable that the *trans* structure cannot be eliminated at higher confidence levels (*e.g.* >99%), thus any model considered must include the possibility of selecting this structure.

One possible source of error in the COOH moiety involves misplacement of the acidic hydrogen. Hydrogen disorder is suggested from the single crystal X-ray structure of the C10 and C12 *n*-alkyl acids in form C where C–O and C=O bond lengths are found to be similar.[13] In contrast, the C11 and C13 acids exhibit C–O and C=O bond lengths more typical of a single and double bond and a localized COOH hydrogen. Disorder in the even numbered acids may involve either the occurrence of both *cis* and *trans* conformations in different parts of the lattice (static disorder) or the presence of COOH hydrogens that can transfer between partners in the dimer over time in a dynamic process. The previous X-ray analyses of lauric acid phase C[12,13] were unable to unambiguously assign the hydrogen position. Here, static disorder is rejected as a possibility because only a single COOH resonance is observed experimentally (see Fig. 2). Two signals would likely be observed in a $^{13}$C isotropic (1D) spectrum of a sample with static disorder.

An infrared spectroscopy study on lauric acid phase C previously identified both the *cis* and *trans* conformations in the solid and measured the ratio as a function of temperature.[52,53] However, this study failed to distinguish static from dynamic disorder and designated the structures only as *cis* or *trans*, providing only rough estimates of hydrogen position. Solid-state NMR has the potential to provide a more accurate position for the disordered hydrogen and to gauge differences in hydrogen bond strength between the disordered and ordered acids.

The dynamic disorder in lauric acid was characterized using a theoretical approach that considers a variety of positions for the COOH proton. A model was created by preparing a pair of butyric acid molecules hydrogen bonded in the head-to-head $R_2^2(8)$ arrangement[54] found in the crystal structure of lauric acid and many other *n*-alkyl acids. Additivity rules predict that substituents beyond the γ-position in carboxylic acids will have a very small influence on $^{13}$COOH shift,[55] thus, truncating lauric acid to butyric acid is unlikely to introduce significant errors. Moreover, prior SSNMR work has demonstrated that $^{13}$C tensors computed from such COOH dimers are comparable in accuracy to those described herein obtained from lattice-including calculations (*i.e.* GIPAW) on model structures.[56] Here, the dimeric model was preferred over GIPAW for two reasons. First, the butyric acid dimer provides a general model applicable to all *n*-alkyl acids involved in $R_2^2(8)$ hydrogen bonding. Second, this model includes only 12 non-hydrogen atoms and is therefore computationally inexpensive, allowing a large variety of candidate structures to be evaluated. All non-hydrogen atom positions in the dimeric model were defined using bond distances and angles from lauric acid's single crystal structure. The C–H hydrogens were placed in positions obtained from the CASTEP refinement. A series of candidate

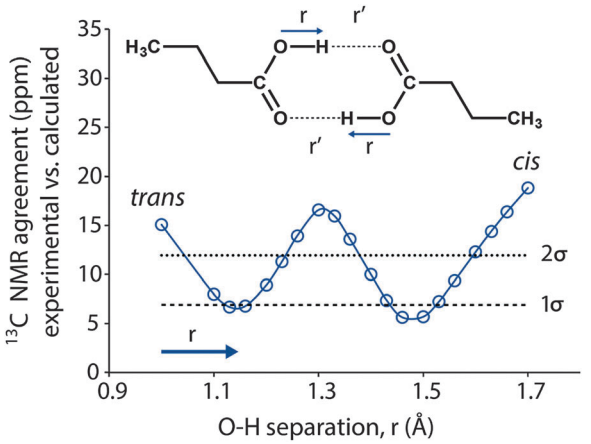


Fig. 4 The agreement between experimental and computed $^{13}$C principal values for the COOH in lauric acid *versus* O–H separation distances. Both the *cis* and *trans* structures with a hydrogen located at a distance similar to that found in neutron diffraction ($r$ = 1.0 Å) are rejected as feasible models at >98% confidence. Two high probability locations for the hydrogen are identified at O–H distances of $r$ = 1.16 ± 0.02 Å and 1.46 ± 0.04 Å. This outcome indicates a hydrogen that is dynamically disordered over two sites on the NMR timescale.

structures were then generated by lengthening each O–H bond in the dimer from an initial separation of $r$ = 1.0 Å in steps varying in size from 0.03 to 0.1 Å to a final separation of 1.7 Å. The initial structure corresponds to the *trans* conformation with an O–H bond length matching the neutron diffraction value in similar compounds.[57] The final 1.7 Å separation mimics the *cis* orientation. At each of the hydrogen position, $^{13}$C tensors were computed at the B3PW91/D95** level of theory. This approach has been employed previously by others and found to give accurate results.[58,59] The agreement with experimental data is shown in Fig. 4 and indicates that hydrogen's environment is characterized by two sites separated by an energy barrier that allows the hydrogen to sample each position on the NMR timescale. The best agreement is achieved at O–H distances of $r$ = 1.16 ± 0.02 and $r$ = 1.46 ± 0.04 Å. To ensure that the dimeric model was valid, a similar analysis was performed with lattice-including methods using lauric acid's crystal structure. These results are included as ESI† and demonstrate that nearly identical O–H distances are selected as the most probable structures. While O–H bond lengths longer than 1.0 Å (*i.e.* the prototypical value found by neutron diffraction)[60] are less commonly encountered, hydrogen disorder is carboxyl dimers is well known from experimental diffraction data.[61–65] Our analysis indicates that lauric acid phase C belong to this class of hydrogen disordered solids.

The proposal for disordered hydrogens implies an energy barrier between the two positions. The height of this energy barrier was evaluated by computing the energy at each point using CASTEP (PBE/ultrafine) and was found to be 36.7 kJ mol$^{-1}$. A list of energy at each point and Boltzmann populations is included as ESI.† This energy barrier is significantly larger than RT at room temperature, suggesting that proton transfer in lauric acid occurs through a tunneling process rather than

classical hopping. These calculations predict energy minima at O–H separations of $r$ = 1.04 Å and 1.60 Å corresponding to O–H bond lengths of 1.04 Å and 1.12 Å for the *trans* and *cis* structures, respectively. It is notable that these lengths which are slightly longer than the value of 1.0 Å expected for localized hydrogens.[60] The predicted bond lengths generally agree with the NMR/DFT values but are consistently shorter by an average of 0.13 Å.

Prior work has demonstrated that benzoic acid also forms hydrogen bonds in an $R_2^2(8)$ arrangement and that COOH proton transfer occurs through coherent tunneling.[66,67] Moreover, benzoic acid's $^{13}$COOH principal values have been measured[68] and are similar to those reported here for lauric acid. Perhaps the most relevant metric for comparing $^{13}$COOH tensors is $\delta_{11}$–$\delta_{22}$ because this value has been shown to be strongly correlated with O–H bond length.[58] Such a comparison yielded $\delta_{11}$–$\delta_{22}$ values of 39 and 36 ppm for lauric acid and benzoic acid, respectively. This strong similarity between $^{13}$COOH tensors indicates a similar electronic environment at the COOH moieties of these acids and suggests that tunneling makes a key contribution to hydrogen disorder in lauric acid, phase C.

These tunneling results taken together with the observation of a single $^{13}$COOH isotropic resonance and the fit to the dimer model (Fig. 4) suggests a dynamic hydrogen transfer that occurs through tunneling between the two COOH sites in lauric acid phase C. Thus the measured $^{13}$COOH shift tensor likely represents a weighted average of the $r$ = 1.16 Å and 1.46 Å structures. The rmds of such an averaged structure *versus* experiment is 5.6 ppm, a value statistically indistinguishable from the two minima in Fig. 4.

Another kind of evidence also supports the contention that lauric acid's hydrogen is dynamically disordered. Prior work by Gu *et al.*[69] demonstrated that $COO^-$ and COOH groups in amino acids could be distinguished by their $^{13}$C principal values. A summary of typical tensor values for COOH and $COO^-$ moieties measured in 74 amino acids and peptides is given in Table 2 together with principal values measured at C1 in lauric acid. These data show a close match between the typical $COO^-$ tensors and C1 of lauric acid. However, elemental analysis of phase C measuring %C, %H and %O unambiguously demonstrates that lauric acid contains the COOH functional group (see Experimental). These data indicate that the electronic environment at lauric's COOH is very similar to that found in $COO^-$ groups. Proton disorder appears to lessen the difference between C–O and C=O bond lengths. A correlation between the difference in these bond lengths (*i.e.* C–O minus C=O) and O–H bond length has previously been predicted by Facelli *et al.*[58] This early work also predicted a decrease in the magnitude of $\delta_{11}$–$\delta_{22}$ as O–H bond length increased, an outcome that is observed in lauric acid. Thus the prediction of COOH hydrogen disorder explains the similarity between lauric acid's $^{13}$C COOH data and the $COO^-$ data in amino acids reported previously.[69]

It has been known since 1877[70] that *n*-alkyl carboxylic acids display alternation in their melting points between odd and even numbered acids. Considerable effort has focused on explaining this difference.[71–77] One unvarying feature of all these explanations is the assumption that the hydrogen bonding at the COOH position is of equal strength in both even and odd numbered acids. One way to evaluate hydrogen bond strength is to measure the $^1$H shift in the COOH moiety. It is well known that $^1$H shifts in O–H···O moieties in the range of 12–21 ppm indicate strong hydrogen bonding with higher frequency shifts indicating stronger hydrogen bonding.[78] A $^1$H spectrum of lauric acid exhibited a $COO^1H$ resonance at 13.6 ppm, consistent with moderately strong hydrogen bonding. Unfortunately, all attempts to measure a similar $^1$H spectrum of undecanoic acid phase C′ were unsuccessful because the high spinning speeds needed for analysis (*i.e.* 25–30 kHz) appeared to melt the sample based upon the unusually narrow $^1$H lines observed upon spinning. This outcome cannot easily be avoided by decreasing temperature because phase C′ changes phase at 17.2 °C. To overcome this limitation, a second analysis was included involving computing $^1$H shifts for the various disordered model structures.

The computed shifts (described above) for the butyric acids model structures include $^1$H isotropic and tensor principal values for all disordered structures. A comparison of calculated isotropic shifts is given in Fig. 5 and indicates that hydrogen disordered structures have higher frequency shifts and thus stronger hydrogen bonds. The strongest hydrogen bonding occurs for a hydrogen positioned at an equal distance from each oxygen atom (*i.e.* $r$ = 1.3 Å). This prediction is consistent with prior studies of very strong O–H···O hydrogen bonds that find hydrogens in such bonds equally positioned between

Table 2 Typical chemical shift tensor principal values[a] at $^{13}$COOH and $^{13}COO^-$ moieties measured in 74 amino acids compared to tensors from lauric acid, phase C

| | $\delta_{11}$ | $\delta_{22}$ | $\delta_{33}$ | $\delta_{iso}$ |
|---|---|---|---|---|
| COOH | 257 ± 6 | 158 ± 18 | 109 ± 8 | 175 ± 6 |
| $COO^-$ | 241 ± 4 | 183 ± 18 | 108 ± 4 | 177 ± 6 |
| C1 (lauric acid, phase C) | 238.8 | 199.4 | 107.6 | 181.9 |

[a] Average values are obtained from 31 COOH and 43 $COO^-$ moieties.

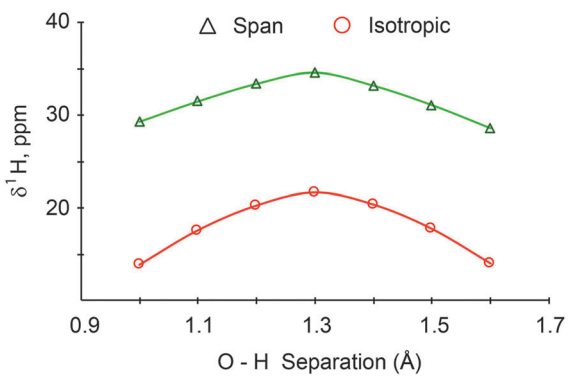


Fig. 5 A comparison of calculated isotropic shifts (1/3 × [$\delta_{11}$ + $\delta_{22}$ + $\delta_{33}$]) and spans ($\delta_{11}$–$\delta_{33}$) for the COOH hydrogen at different O–H bond lengths. These data both support the conclusion that proton disorder in the COOH creates stronger hydrogen bonds. All data points were computed at the B3LYP/D95** level of theory.

 

oxygen atoms in bonds that exhibit significant covalent character.[79] Further support for the conclusion that disorder creates stronger hydrogen bonds comes from the computed $^1$H shift tensor data. It is known that the span (*i.e.* $\delta_{11}$–$\delta_{33}$) of $^1$H shift tensors in X–$^1$H···Y bonds are sensitive to hydrogen bond strength with larger spans indicating stronger hydrogen bonding.[80] For the dimeric model structure considered, the span increases as the O–H bond length increases with a maximum value observed at $r$ = 1.3 Å (Fig. 5). Thus the data on span also indicate that stronger hydrogen bonding results from proton disorder.

Overall, these analyses of $^1$H shifts suggest that lauric acid phase C has stronger hydrogen bonding than undecanoic acid phase C′. However, predictions regarding the magnitude of this difference cannot be made from the present data. We note that a more quantitative approach is often performed in order to compute hydrogen bond strength involving comparing the energy for the dimer in the optimized hydrogen bonding position against isolated monomers.[81] In the current study such calculations are infeasible because the O–H bond lengths in the disordered structures do not represent stationary points.

The above discussion on differences in COOH hydrogen disorder in odd and even numbered acids is based primarily on bond length differences at C–O and C═O in diffraction structures. These differences (*i.e.* C–O minus C═O) are said to be observed in odd and even numbered acids from C6 to C15[12] with the odd acids having larger values on average (Fig. 6). However, these differences are consistently smaller than the ideal value of 0.10 Å found in localized COOH moieties[57] and in some cases (*e.g.* C9/C10) are negligible. It is therefore desirable to look at other evidence to more fully establish that even and odd numbered acids differ in hydrogen disorder and hydrogen bond strength. Accordingly, the $^{13}$COOH tensor principal values were measured for the phase of undecanoic acid that occurs immediately before melting (*i.e.* phase C′)[15] using an approach described in Experimental (Table 3). The agreement between undecanoic acid's experimental COOH tensors and computed values from the dimeric model structure described previously is illustrated in Fig. 7. These data establish that undecanoic acid's COOH hydrogen is localized with an O–H bond length

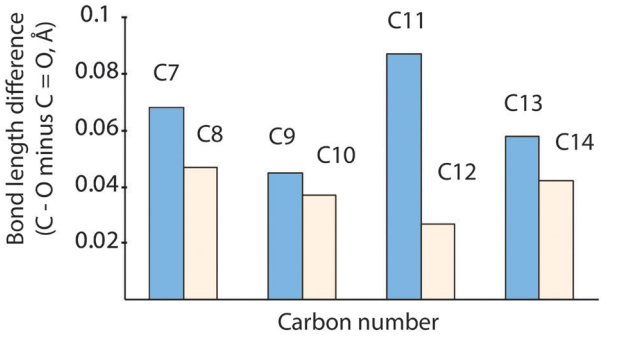


Fig. 6 Differences between C–OH and C═O bond lengths in C7 to C14 *n*-alkyl monocarboxylic acids. All bond lengths are taken from X-ray single crystal data.[13]

Table 3 Experimental $^{13}$C chemical shift tensor principal values (ppm) for undecanoic acid, phase C′

| Position | $\delta_{11}$ | $\delta_{22}$ | $\delta_{33}$ | $\delta_{iso}$ |
|---|---|---|---|---|
| COOH | 250 | 160 | 111 | 173.8 |

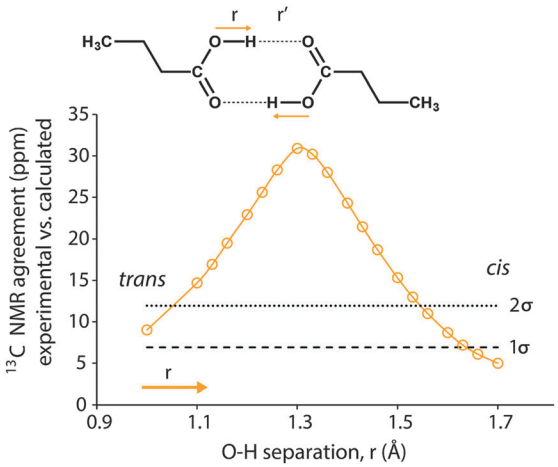


Fig. 7 The agreement between experimental and computed $^{13}$C principal values for the COOH in undecanoic acid *versus* O–H separation distances. The *cis* structure with a localized hydrogen at an O–H separation of 1.70 ± 0.07 Å gives best agreement with experimental $^{13}$C tensor data. This minimum corresponds to an O–H bond length of 1.02 Å. Structures having a disordered hydrogen are rejected at >95% statistical confidence.

of 1.02 ± 0.07 Å and a Cβ–Cα–C═O moiety in a *cis* orientation. This prediction agrees with the single crystal X-ray diffraction structure where a *cis* conformation is observed. Our prior discussion of hydrogen bonding in the dimer model and $^1$H chemical shifts indicates that localized $R_2^2(8)$ hydrogen bonds are weaker than delocalized bonds. Thus significant differences in hydrogen disorder and hydrogen bond strength are observed between lauric and undecanoic acid. Admittedly, the nature of this comparison is limited and a more extensive comparison involving other *n*-alkyl acids is desirable.

It is interesting to speculate on why COOH hydrogen disorder is observed in even but not in odd numbered acids. Several studies have demonstrated that the key difference between even and odd *n*-alkyl acids lies is the packing density.[12,13,76] Even acids are able to achieve favorable packing at the methyl–methyl interface that occurs between bilayers. In contrast, odd acids show a void volume between methyl groups that is between 17 and 27% larger than that found in even acids.[13] At other points in the lattice, the packing efficiency for odd and even acids is similar. Prior work by Bond[13] has established that even acids are able to maintain this favorable methyl–methyl packing by translating the dimeric hydrogen bonded pairs along the *n*-alkyl direction relative to an adjacent dimer pair to relieve repulsive O···O contacts that would occur if optimal packing were enforced. This translation also allows neighboring *n*-alkyl chains to move closer to maximize the dispersion forces. Perhaps more importantly, this decrease in O···O repulsion appears to be a crucial factor in allowing hydrogen disorder to develop. Prior theoretical

work suggests that the key factor in developing low-barrier hydrogen bonds capable of proton disorder is the formation of a double-well hydrogen bond having degenerate or near-degenerate energy minima.[82] Matched p$K_a$'s for the conjugate bases of the two moieties involved in the hydrogen bond can help achieve this degeneracy, but this match appears to not be strictly required.[82] In even numbered acids this disorder creates more dense solids with higher melting points due to both increased dispersion interactions in the *n*-alkyl chains and stronger hydrogen bonding. In odd numbered acids, this translation process is prohibited by the dimer geometry and optimization of the unfavorable O···O intermolecular interactions and energetically favorable *n*-alkyl chain associations is not possible. This important difference results in an inability to create the degenerate double-well minima needed for proton disorder. This structural constraint in odd numbered acids creates localized O–H bonds that form weaker hydrogen bonds and less favorable dispersion interaction in the *n*-alkyl chains. Taken together, these changes create lower melting solids for odd numbered acids.

## Conclusions

The work described herein demonstrates that the accurate SSNMR characterization of COOH hydrogen position and the detection of dynamic disorder in lauric acid resolves an ambiguity in prior crystal structures. The refinement process includes a combination of techniques with CASTEP lattice-including DFT first relaxing the majority of atomic positions followed by manual adjustment of a single hydrogen to further alter structure near C1 where the agreement between experiment and theory remains poor. This study also invites a reevaluation of the almost universally held assumption that all $R_2^2(8)$ hydrogen-bonding interactions in *n*-alkyl acids are the same. The SSNMR and DFT modeling evidence supports the presence of a stronger $R_2^2(8)$ hydrogen bond in lauric acid than is found in undecanoic acid. A variety of other data (*e.g.* X-ray bond lengths and melting points) suggest that similar differences in COOH structure and hydrogen bond strength occur in other odd and even numbered acids. This analysis thus provides a new and significant piece of information that should further improve understanding of the behavior of *n*-alkyl acids. It is noteworthy that several other classes of compounds (*e.g.* α,ω-alkanediols,[83] α,ω-alkanediamines,[83] α,ω-alkanedithiols,[84] and α,ω-alkanedicarboxylic acids[85]) have also been found to exhibit alternating density and melting point behavior. Solid-state NMR studies aimed at improving hydrogen positions and more fully elucidating the role of hydrogen disorder may also prove beneficial in understanding these materials.

## Acknowledgements

This work was supported by National Science Foundation under CHE-1455159 to J. K. H. We acknowledge the University of Central Florida Stokes Advanced Research Computing Center for providing computational resources and support that have contributed to results reported herein, URL http://webstokes.ist.ucf.edu.

## Notes and references

1 J. Metz and M. Lassener, *Ann. N. Y. Acad. Sci.*, 1996, **792**, 82.
2 K. G. Berger and N. A. Idris, *J. Am. Oil Chem. Soc.*, 2005, **82**, 775.
3 F. M. Dayrit, *J. Am. Oil Chem. Soc.*, 2015, **92**, 1.
4 M. J. Abdul Afig, R. Abdul Rahman, Y. B. Cheman, H. A. Al-Kahtani and T. S. T. Mansor, *Int. Food Res. J.*, 2013, **20**, 2035.
5 B. J. German, *Sci. Aliments*, 2008, **28**, 176.
6 C. L. Fisher, D. R. Blanchette, R. Derek, K. A. Brogden, D. V. Dawson, D. R. Drake, J. R. Hill and P. W. Wertz, *Biochim. Biophys. Acta, Mol. Cell Biol. Lipids*, 2014, **1841**, 319.
7 H. Thormar and H. Hilmarsson, *Chem. Phys. Lipids*, 2007, **150**, 1.
8 T. R. Lomer, *Acta Crystallogr.*, 1963, **16**, 984.
9 M. Goto and E. Asada, *Bull. Chem. Soc. Jpn.*, 1978, **51**, 70.
10 T. R. Lomer and R. M. Spanswick, *Acta Crystallogr.*, 1961, **14**, 312.
11 E. Von Sydow, *Acta Chem. Scand.*, 1956, **10**, 1.
12 E. Moreno-Calvo, G. Gbabode, R. Cordobilla, T. Calvet, M. A. Cuevas-Diarte, P. Negrier and D. Mondieig, *Chem. – Eur. J.*, 2009, **15**, 13141.
13 A. D. Bond, *New J. Chem.*, 2004, **28**, 104.
14 V. Vand, W. M. Morley and T. R. Lomer, *Acta Crystallogr.*, 1951, **4**, 324.
15 For even-numbered acids, the high-temperature phase is referred to as the C form. For odd-numbered acids the high-temperature polymorph is called the C′ or C″ phase.
16 A. Sari and K. Kaygusuz, *Energy Convers. Manage.*, 2002, **43**, 863.
17 A. Sari, *Appl. Therm. Eng.*, 2003, **23**, 1005.
18 A. W. Ralston, *Fatty Acids and Their Derivatives*, Wiley, New York, 1948.
19 S. E. Ashbrook, M. Cutajar, C. J. Pickard, R. I. Walton and S. Wimperis, *Phys. Chem. Chem. Phys.*, 2008, **10**, 5754.
20 M. Profeta, F. Mauri and C. J. Pickard, *J. Am. Chem. Soc.*, 2003, **125**, 541.
21 D. H. Brouwer, I. L. Moudrakovski, R. J. Darton and R. E. Morris, *Magn. Reson. Chem.*, 2010, **48**, S113.
22 E. Salager, R. S. Stein, C. J. Pickard, B. Elena and L. Emsley, *Phys. Chem. Chem. Phys.*, 2009, **11**, 2610.
23 J. C. Johnston, R. J. Iuliucci, J. C. Facelli, G. Fitzgerald and K. T. Mueller, *J. Chem. Phys.*, 2009, **131**, 144503.
24 J. K. Harper, R. J. Iuliucci, M. Gruber and K. Kalakewich, *CrystEngComm*, 2013, **15**, 8693.
25 K. Kalakewich, R. Iuliucci and J. K. Harper, *Cryst. Growth Des.*, 2013, **13**, 5391.
26 J. Czernek, T. Pawlak, M. J. Potrzebowski and J. Brus, *Chem. Phys. Lett.*, 2013, **555**, 135.
27 T. Pawlak, M. Jaworska and M. J. Potrzebowski, *Phys. Chem. Chem. Phys.*, 2013, **15**, 3137.

 

28 R. Witter, U. Sternberg and A. S. Ulrich, *J. Am. Chem. Soc.*, 2006, **128**, 2236.
29 K. Kalakewich, R. Iuliucci, K. T. Mueller, H. Eloranta and J. K. Harper, *J. Chem. Phys.*, 2015, **143**, 194702.
30 M. D. Segall, P. J. D. Lindan, M. J. Probert, C. J. Pickard, P. J. Hasnip, S. J. Clark and M. C. Payne, *J. Phys.: Condens. Matter*, 2002, **14**, 2717.
31 R. Witter, U. Sternberg, S. Hesse, T. Kondo, F.-T. Koch and A. S. Ulrich, *Macromolecules*, 2006, **39**, 6125.
32 Y. Nishiyama, J. Sugiyama, H. Chanzy and P. Langan, *J. Am. Chem. Soc.*, 2003, **125**, 14300.
33 T. Pawlak and M. J. Potrzebowski, *J. Phys. Chem. B*, 2014, **118**, 3298.
34 D. W. Alderman, G. McGeorge, J. Z. Hu, R. J. Pugmire and D. M. Grant, *Mol. Phys.*, 1998, **95**, 1113.
35 A. E. Bennett, C. M. Rienstra, M. Auger, K. V. Lakshmi and R. G. Griffin, *J. Chem. Phys.*, 1995, **103**, 6951.
36 G. McGeorge, J. Z. Hu, C. L. Mayne, D. W. Alderman, R. J. Pugmire and D. M. Grant, *J. Magn. Reson.*, 1997, **129**, 134.
37 R. C. F. Schaake, J. C. van Miltenburg and C. G. De Kruif, *J. Chem. Thermodyn.*, 1982, **14**, 763.
38 B.-J. van Rossum, C. P. de Groot, V. Ladizhansky, S. Vega and H. J. M. de Groot, *J. Am. Chem. Soc.*, 2000, **122**, 3465.
39 B. M. Fung, A. K. Khitrin and K. Ermolaev, *J. Magn. Reson.*, 2000, **142**, 97.
40 B.-J. van Rossum, H. Förster and H. J. M. de Groot, *J. Magn. Reson.*, 1997, **124**, 516.
41 B. G. Pfrommer, M. Cote, S. G. Louie and M. L. Cohen, *J. Comput. Phys.*, 1997, **131**, 233.
42 C. J. Pickard and F. Mauri, *Phys. Rev. B: Condens. Matter Mater. Phys.*, 2001, **63**, 245101.
43 J. K. Harper, in *Encyclopedia of NMR*, ed. D. M. Grant and R. K. Harris, Wiley, Chichester, 2002, vol. 9, pp. 589–597.
44 D. H. Brouwer, *J. Am. Chem. Soc.*, 2008, **130**, 6306.
45 R. A. Olsen, J. Struppe, D. W. Elliott, R. J. Thomas and L. J. Mueller, *J. Am. Chem. Soc.*, 2003, **125**, 11784.
46 C. Luchinat, G. Parigi, E. Ravera and M. Rinaldelli, *J. Am. Chem. Soc.*, 2012, **134**, 5006.
47 J. K. Harper and R. J. Iuliucci, in *Encyclopedia of Analytical Chemistry*, ed. R. A. Meyers, Wiley, New York, 2014, pp. 1–37.
48 I. Nahringbauer, *Acta Crystallogr., Sect. B: Struct. Crystallogr. Cryst. Chem.*, 1978, **34**, 315.
49 I. Nahringbauer, *Acta Chem. Scand.*, 1970, **24**, 453.
50 T. M. Duncan and R. W. Vaughan, *J. Catal.*, 1981, **67**, 49.
51 A. Pines, M. G. Gibby and J. S. Waugh, *Chem. Phys. Lett.*, 1972, **15**, 373.
52 S. Hayashi and J. Umemura, *J. Chem. Phys.*, 1975, **63**, 1732.
53 S. Hayashi, J. Umemura and R. Nakamura, *J. Mol. Struct.*, 1980, **69**, 123.
54 J. Bernstein, R. E. Davis, L. Shimoni and N.-L. Chang, *Angew. Chem., Int. Ed. Engl.*, 1995, **34**, 1555.
55 E. Pretsch, P. Bühlmann and M. Badertscher, *Structural Determination of Organic Compounds*, Springer-Verlag, Berlin, 2009.
56 J. K. Harper, D. H. Barich, J. Z. Hu, G. A. Strobel and D. M. Grant, *J. Org. Chem.*, 2003, **68**, 4609.
57 L. Lieserowitz, *Acta Crystallogr., Sect. B: Struct. Crystallogr. Cryst. Chem.*, 1976, **32**, 775.
58 J. C. Facelli, Z. Gu and A. McDermott, *Mol. Phys.*, 1995, **86**, 865.
59 M. Ilczyszyn, D. Godzisz, M. M. Ilczyszyn and K. Mierzwicki, *Chem. Phys.*, 2006, **323**, 231.
60 P.-G. Jonsson, *Acta Crystallogr., Sect. B: Struct. Crystallogr. Cryst. Chem.*, 1971, **27**, 893.
61 D. J. Duchamp and R. E. Marsh, *Acta Crystallogr., Sect. B: Struct. Crystallogr. Cryst. Chem.*, 1969, **25**, 5.
62 M. G. Takwale and L. M. Pant, *Acta Crystallogr., Sect. B: Struct. Crystallogr. Cryst. Chem.*, 1971, **27**, 1152.
63 M. Bailey and C. J. Brown, *Acta Crystallogr.*, 1967, **22**, 387.
64 H. H. Sutherland, *Acta Crystallogr., Sect. B: Struct. Crystallogr. Cryst. Chem.*, 1969, **25**, 171.
65 H. H. Sutherland, *Acta Crystallogr., Sect. B: Struct. Crystallogr. Cryst. Chem.*, 1970, **26**, 1217.
66 M. Neumann, D. F. Brougham, C. J. McGloin, M. R. Johnson, A. J. Horsewill and H. P. Trommsdorff, *J. Chem. Phys.*, 1998, **109**, 7300.
67 A. Oppenländer, C. Rambaud, H. P. Trommsdorff and J.-C. Vial, *Phys. Rev. Lett.*, 1989, **63**, 1432.
68 G. J. Rees, S. D. Day, A. Lari, A. P. Howes, D. Iuga, M. B. Pitak, S. J. Coles, T. L. Threlfall, M. E. Light, M. E. Smith, D. Quigley, J. D. Wallis and J. V. Hanna, *CrystEngComm*, 2013, **15**, 8823.
69 Z. Gu, R. Zambrano and A. McDermott, *J. Am. Chem. Soc.*, 1994, **116**, 6368.
70 A. Baeyer, *Ber. Dtsch. Chem. Ges.*, 1877, **10**, 1286.
71 K. Larson, *J. Am. Oil Chem. Soc.*, 1966, **43**, 559.
72 H. Pauly, *Z. Anorg. Chem.*, 1922, **119**, 271.
73 A. Muller, *Proc. R. Soc. London, Ser. A*, 1929, **124**, 317.
74 T. Malkin, *J. Chem. Soc.*, 1931, 2796.
75 A. E. Bailey, *Melting and solidification of fats*, Interscience Publishers Inc., New York, 1950.
76 E. J. Gorin, J. Walter and H. Eyring, *J. Am. Chem. Soc.*, 1939, **61**, 1876.
77 D. Chapman, *Chem. Rev.*, 1962, **62**, 433.
78 A. McDermott and C. F. Ridenour, *Encyclopedia of NMR*, Wiley, Sussex, 1996.
79 P. Gilli, V. Bertolasi, V. Ferretti and g. Gilli, *J. Am. Chem. Soc.*, 1994, **116**, 909.
80 J. K. Harper, in *NMR Crystallography*, eds. R. K. Harris, R. E. Wasylishen and M. J. Duer, Wiley, Chichester, 2009, p. 117.
81 W. Koch and M. C. Holthausen, *A Chemists Guide to Density Functional Theory*, Wiley-VHC, New York, 2000.
82 M. Garcia-Viloca, A. Gonzalez-Lafont and J. M. Lluch, *J. Phys. Chem. A*, 1997, **101**, 3880.
83 V. R. Thalladi, R. Boese and H.-C. Weiss, *Angew. Chem., Int. Ed.*, 2000, **39**, 918.
84 V. R. Thalladi, R. Boese and H.-C. Weiss, *J. Am. Chem. Soc.*, 2000, **122**, 1186.
85 V. R. Thalladi, M. Nüsse and R. Boese, *J. Am. Chem. Soc.*, 2000, **122**, 9227.